Eur. Phys. J. B **41**, 177–184 (2004)
DOI: 10.1140/epjb/e2004-00307-6

THE EUROPEAN PHYSICAL JOURNAL B

Microwave propagation in two dimensional structures using lossy cylindrical glass rods

E.D.V. Nagesh[1], G. Santosh Babu[1], V. Subramanian[1,a], V. Sivasubramanian[2], and V.R.K. Murthy[1]

[1] Microwave Laboratory, Department of Physics, Indian Institute of Technology, Madras, Chennai, 600 036, India
[2] Material Science Division, Indira Gandhi Centre for Atomic Research, Kalpakkam, 603 102, India

Received 26 September 2003 / Received in final form 26 April 2004
Published online 12 October 2004 –

Abstract. Two dimensional microwave band gap structures have been constructed using lossy cylindrical glass samples ($\varepsilon' = 5.5$ and $\varepsilon'' = 0.1$). The power transmission spectra observed between 10 and 20 GHz for both square and triangular structures with three different lattice spacing (2.5, 1.4 and 0.9 cm) are explained in terms of the lattice spacing, filling fraction and loss tangent. The experimental results and the theoretical values agree well for the structures having higher filling fraction. Also, the values predicted from the scaling procedure agree well with the experimental values. The appearance of acceptor modes due to the introduction of defects in these structures is also reported.

PACS. 41.20.Jb Electromagnetic wave propagation; radiowave propagation – 42.25.Fx Diffraction and scattering

1 Introduction

The propagation of electromagnetic radiation through a periodic arrangement of dielectric material has attracted many researchers [1–5] and has stimulated intensive fundamental and applied research. These structures called Photonic Band Gap (PBG) structures or photonic crystals (PCs) can be constructed over a wide frequency range from the microwave to the visible region. PBG structures are used for devices such as filters, reflectors, waveguides, antennas, optical switches etc. The waveguides using PBG structures are efficient compared to conventional waveguides due to a wide range of allowed frequencies and zero loss near the bends [6]. The electromagnetic waves traveling through such structures experience a periodic variation of dielectric constant similar to the periodic potential energy of an electron in an atomic crystal. Therefore, like the electronic state in an atomic crystal, the photonic state in a photonic crystal can be classified into bands and gaps, the frequency range over which the photons are allowed or forbidden respectively to propagate in the medium. It is well known that any periodic structure with a length scale comparable to that of the wavelength of the particle would coherently scatter and form energy bands in a medium that provides a periodic scattering potential [7]. In the PBG structures the waves are Bragg scattered and if the scattered waves from different layers interfere destructively, they give rise to a gap.

The PBG structures are characterized by three important parameters viz. periodicity of the geometric arrangement, dielectric contrast and filling fraction. The periodicity of the geometric arrangement is decided by the wavelength of the electromagnetic spectrum of interest. In the microwave region, the periodicity is expected to be between 0.3 mm and 100 cm. McCall and Platzman [8] utilized alumina rods in the square periodicity with a lattice spacing of 1.27 cm for observing a gap around 10–12 GHz. Apart from the periodicity of the dielectric constant, it is necessary to have a good dielectric contrast (ratio between the dielectric constant of sample and background material) between the background material and the sample used in the structure [9]. Interestingly, this degree of contrast varies with the dimension of the structure. Yablonovitch and Gmitter [10] suggested that the contrast should be nearly 3.5 for a 3-dimensional structure for the formation of band gap. The width of the gap depends on the filling fraction (the fractional volume occupied by the dielectric samples to that of the background material in an unit cell) of the given structure. It is important to have an optimum filling fraction for the maximum width of the band gap. This optimum filling fraction varies with the dielectric contrast [11].

Most of the theoretical formulations for the band gap calculations involve a non-lossy medium. But in reality, as all the materials absorb some radiation, the dielectric loss of the material should also be taken into consideration. The theoretical analysis by Sigalas et al. [12] shows an increase in the width of the gap with the dielectric loss

[a] e-mail: manianvs@iitm.ac.in

while the position of the gap remains unchanged. Moreover, there is a reduction in the transmitted power levels due to absorption.

As in the case of defects in electronic crystals, one can have defects in PBG structures also. These defects can be created either by removing or adding a material into the lattice, thereby disturbing the periodicity. This may result in the appearance of extra modes in the forbidden frequency range or a change in the power levels. Depending on the position of the defect and the number of defects that are created, the change in the power levels is either more or less. By addition of material, if a defect mode is created, then it is referred to as a donor mode and if the material is removed to form a defect mode, it is referred to as an acceptor mode [13]. Defects can also be created either by changing the refractive index or by changing the size of the rods (in diameter) or even by removing the rods [14].

As mentioned earlier, while several literatures deal with the non-lossy medium for the PBG structures at microwave frequency, only few are available on the analysis of the structure with loss [12,15]. Moreover, to understand the effect of loss on the PBG structure, it is necessary to compare the theoretical analysis with the actual experimental data. Therefore, an effort has been made to construct a PBG structure suitable for the microwave frequency, known as Microwave Band Gap (MBG) structure, using a lossy dielectric material. In this paper, we report the transmission spectra obtained between 10 and 20 GHz for two dimensional square and triangular MBG structures using glass as the lossy dielectric medium ($\varepsilon_{\mathrm{r}}' = 5.5$ and $\varepsilon_{\mathrm{r}}'' = 0.1$). The results are compared with the theoretical data obtained using plane wave method. The paper also discusses the results obtained for the above structures with the introduction of acceptor defects.

2 Experimental set-up

A microwave vector network analyzer (HP 8720A) was used to obtain the S_{12} parameter between 10 and 20 GHz with the help of two horn antennas kept on either side of the structure. The antennas were separated by a distance of 50 cm. The fringe effects of the electric field were assumed to be minimum. Initially, the S_{12} parameter was normalized without any structure between the antennas. For all the experiments, an E-polarized beam (with electric field parallel to the length of the rod) was used.

The structure was prepared by cylindrical glass rods of diameter 0.414 cm and length 15 cm. The dielectric contrast in the present case was 5.5. The square and triangular (hexagonal) structures with three different lattice constants 2.5, 1.4 and 0.9 cm were constructed using 10×10 matrix elements. These matrix arrangements were then placed between the horn antennas and the transmission spectra were recorded. The acceptor mode defect structures were also studied for all the above structures.

3 Theory

Of the many theoretical formulations such as Plane Wave Method for band structure calculations [16] and Transfer Matrix Method for band structure calculations as well as for transmission spectrum [17], we have used the plane wave method because of the simplicity involved in this method. In this method, we assume a lattice consisting of infinitely long, parallel dielectric rods of dielectric constant ε_a, each with a circular cross section of radius R embedded in a background dielectric material of dielectric constant ε_b. We also assume the structure to be infinite though in practice it is limited. The intersections of these rods with a perpendicular plane form the square or triangular lattice. The electromagnetic waves are assumed to propagate in a plane perpendicular to the rods and only E-polarization (electric field parallel to the rods) is considered here.

The Maxwell's equations in frequency domain can be written as

$$\nabla \times \vec{E}(\vec{x}) - \frac{i\omega}{c}\vec{H}(\vec{x}) = 0$$
$$\nabla \times \vec{H}(\vec{x}) + \frac{i\omega}{c}\varepsilon(\vec{x})\vec{E}(\vec{x}) = 0. \quad (1)$$

Using these two equations one can obtain the equation in terms of electric field as

$$\frac{1}{\varepsilon(\vec{x})}\nabla \times \nabla \times \vec{E}(\vec{x}) = \frac{\omega^2}{c^2}\vec{E}(\vec{x}). \quad (2)$$

As the spatial dependence exists only in two dimensions, say, x_1x_2 – plane, we can write

$$\nabla \times \vec{E} = \hat{x}_1\frac{\partial E_3}{\partial x_2} - \hat{x}_2\frac{\partial E_3}{\partial x_1} \quad (3)$$

where E_3 is the component of electric field along $\hat{x}_3$ and

$$\nabla \times \nabla \times E = -\hat{x}_3\left(\frac{\partial^2 E_3}{\partial x_1^2} + \frac{\partial^2 E_3}{\partial x_2^2}\right). \quad (4)$$

Substituting in equation (2) and using

$$E(\vec{x},t) = E_0(\vec{x}|\omega)\ e^{-i\omega t} = (0,0,E_3(\vec{x}|\omega))\ e^{-iwt}, \quad (5)$$
$$H(\vec{x},t) = H_0(\vec{x}|\omega)\ e^{-i\omega t}$$
$$= (H_1(\vec{x}|\omega), H_2(\vec{x}|\omega), 0)\ e^{-i\omega t}, \quad (5a)$$

we obtain the equation for E_3 as

$$\frac{1}{\varepsilon(\vec{x})}\left(\frac{\partial^2}{\partial x_1^2} + \frac{\partial^2}{\partial x_2^2}\right)E_3 + \frac{\omega^2}{c^2}E_3 = 0. \quad (6)$$

Expanding $\varepsilon^{-1}(\vec{x})$ in Fourier space as

$$\frac{1}{\varepsilon(\vec{x}_{||})} = \sum_{\vec{G}_{||}} \hat{K}\left(\vec{G}_{||}\right) e^{i\vec{G}_{||}\cdot\vec{x}_{||}} \quad (6a)$$

where $\vec{G}_{||}$ is a reciprocal lattice vector and $\hat{K}\left(\vec{G}_{||}\right)$ is the Fourier coefficient.

The reciprocal lattice vector $\vec{G}_{||}$ is given by $\vec{G}_{||} = h_1\vec{b}_1 + h_2\vec{b}_2$ where $\vec{b}_1$, $\vec{b}_2$ are the corresponding lattice vectors along $\hat{x}_1$ and $\hat{x}_2$ respectively and h_1, h_2 are integers.

Writing $E_3(\vec{x}|\omega)$ according to Bloch's theorem as $E_3(\vec{x}|\omega) = \sum_{\vec{G}_{||}} B\left(\vec{k}_{||} + \vec{G}_{||}\right) e^{i(\vec{k}_{||}+\vec{G}_{||})\vec{x}}$ we can concentrate on the values of $\vec{k}_{||}$ that are in first Brillouin Zone.

The Fourier coefficients $\hat{K}\left(\vec{G}_{||}\right)$ are given by

$$\hat{K}\left(\vec{G}_{||}\right) = \frac{1}{\varepsilon_a} f + \frac{1}{\varepsilon_b}(1-f), \qquad \text{if} \quad \vec{G}_{||} = 0\,;$$

$$\hat{K}\left(\vec{G}_{||}\right) = \left(\frac{1}{\varepsilon_a} - \frac{1}{\varepsilon_b}\right) f \frac{2J_1\left(|\vec{G}_{||}|R\right)}{|\vec{G}_{||}|R} \qquad \text{if} \quad \vec{G}_{||} \neq 0 \tag{6b}$$

where J_1 is a Bessel function of first kind, f is the filling fraction given by $f = \frac{\pi R^2}{a^2}$ for a square lattice and $f = \frac{2}{\sqrt{3}}\frac{\pi R^2}{a^2}$ for a triangular lattice. where a is the lattice constant.

The equation satisfied by the coefficients $B\left(\vec{k}_{||} + \vec{G}_{||}\right)$ is

$$\sum_{\vec{G}_{||}} \hat{K}\left(\vec{G}_{||} - \vec{G}'_{||}\right) B\left(\vec{k}_{||} + \vec{G}'_{||}\right) \left|\vec{k}_{||} + \vec{G}'_{||}\right|^2 = \left(\frac{\omega^2}{c^2}\right) B\left(\vec{k}_{||} + \vec{G}_{||}\right). \tag{7}$$

To have a symmetrical eigen value problem with real eigen vectors, we can write

$$C\left(\vec{k}_{||} + \vec{G}_{||}\right) = B\left(\vec{k}_{||} + \vec{G}_{||}\right)\left|\vec{k}_{||} + \vec{G}_{||}\right|. \tag{8}$$

Then equation (6) becomes

$$\sum \hat{K}\left(\vec{G}_{||} - \vec{G}'_{||}\right)|\vec{k}_{||} + \vec{G}_{||}||\vec{k}_{||} + \vec{G}'_{||}|\, C\left(\vec{k}_{||} + \vec{G}'_{||}\right) = \left(\frac{\omega^2}{c^2}\right) C\left(\vec{k}_{||} + \vec{G}_{||}\right). \tag{9}$$

For a given vector $\vec{k}_{||}$ and a set of vectors $\vec{G}_{||}$, equation (9) represents an eigen value problem from which we can find the eigen values (ω^2/c^2). The band structures for the wave vector along $\Gamma - \mathrm{X}$ for the square and $\Gamma - \mathrm{M}$ for the triangular lattice were considered to coincide with the measurement direction. The band gap formation between 10 and 20 GHz only were taken into consideration for comparing with experimental results. A typical band structure obtained for 0.9 cm square and triangular lattices are shown in Figures 1 and 2.

It is very well known that PBG structures have no particular length scales and so it is always possible to use the scaling property of the electromagnetic equations to calculate the position of the mid-gap frequency. The theoretical results obtained for the same lattice structure but with different spacing and dielectric constant are compared with the present results by using the scaling property. The methodology of scaling for both lattice spacing and dielectric constant is explained below [9].

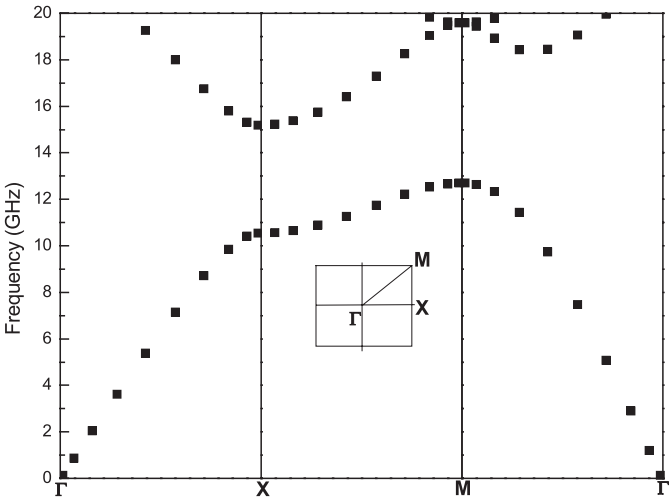

Fig. 1. The band structure of a 0.9 cm square lattice computed using plane wave method. The inset shows the first Brillouin zone for the square lattice.

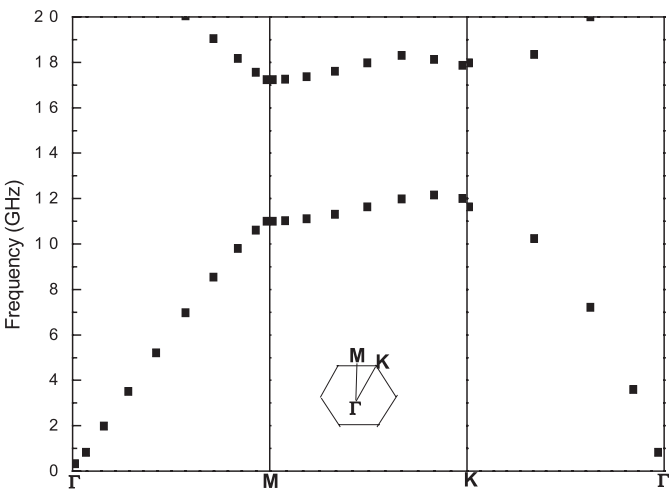

Fig. 2. The band structure of a 0.9 cm triangular lattice computed using plane wave method. The inset shows the first Brillouin zone for triangular lattice.

The master equation for calculating the band gaps can be obtained from Maxwell's equations as

$$\vec{\nabla} \times \left(\frac{1}{\varepsilon(r)}\vec{\nabla} \times \vec{H}(r)\right) = \left(\frac{\omega}{c}\right)^2 \vec{H}(r). \tag{10}$$

If the new lattice parameter is r' ($r' = s_l r$, where s_l is the scale parameter), then equation (10) is modified as

$$s_l\vec{\nabla}' \times \left(\frac{1}{\varepsilon(r'/s_l)} s_l\vec{\nabla}' \times \vec{H}(r'/s_l)\right) = \left(\frac{\omega}{c}\right)^2 \vec{H}(r'/s_l) \tag{11}$$

where $\vec{\nabla}' = \vec{\nabla}/s_l$.

Dividing out the s_l's shows that

$$\vec{\nabla}' \times \left(\frac{1}{\varepsilon'(r')}\vec{\nabla}' \times \vec{H}(r'/s_l)\right) = \left(\frac{\omega}{cs_l}\right)^2 \vec{H}(r'/s_l). \quad (12)$$

This is similar to the equation (10) where the new frequency is scaled by a factor s_l such that $\omega' = \omega/s_l$.

Following the similar procedure one can arrive at the following equation for scaling the dielectric constant

$$\vec{\nabla} \times \left(\frac{1}{\varepsilon'(r)}\vec{\nabla} \times \vec{H}(r)\right) = \left(\frac{s_d\omega}{c}\right)^2 \vec{H}(r) \quad (13)$$

where $\varepsilon'(r)$ is the new dielectric constant ($\varepsilon'(r) = \varepsilon(r)/s_d^2$) and s_d^2 is the scaling factor for dielectric constant. The frequencies are all scaled for this case by s_d such that $\omega' = s_d\omega$. Therefore, by following this procedure one can predict the mid-gap frequency for a given structure from the already available experimental or theoretical data.

4 Results

4.1 Square lattice

In the spectrum obtained with the square lattice of spacing 2.5 cm (filling fraction 2.2%), two sharp gaps as shown in Figure 3 were observed at 10.19 GHz (gap width 0.24 GHz) and 12.39 GHz (gap width 0.3 GHz). Plane wave method predicts only one gap centered at 10.53 GHz with a width of 1.1 GHz.

With a lattice constant of 1.4 cm (filling fraction 6.9%), only one band gap of width 4.2 GHz centered at 17.42 GHz is observed as shown in Figure 4. In this case, plane wave method predicts a gap at 16.42 GHz with a width of 3.46 GHz.

With the lattice constant of 0.9 cm (filling fraction 16.6%), the gap width increases to 4.4 GHz centered at 13.39 GHz as shown in Figure 5. The theoretical prediction by plane wave method points out a gap centered at 12.9 GHz with a width of 4.68 GHz. One can also observe that there is an improvement in the spectrum in terms of gap width as the filling fraction is increased.

Plihal et al. [16] calculated the band structures for a dielectric contrast of 5 and filling fraction of 0.189 for a square lattice using the plane wave expansion method. Using the scaling methodology for dielectric constant as well as lattice parameter, the calculations were performed for the midgap frequencies for the three lattice parameters. Accordingly, the midgap frequency for 2.5 cm lattice was calculated as 4.85 GHz. Since our scanned frequency range starts from 10 GHz onwards, this gap could not be observed at this frequency. For 1.4 cm lattice structure, the gap should appear at 8.65 GHz, which also could not be observed within the scanned frequency range. For 0.9 cm lattice, the midgap frequency observed at around 13.39 GHz agreed well with the expected value of 13.45 GHz.

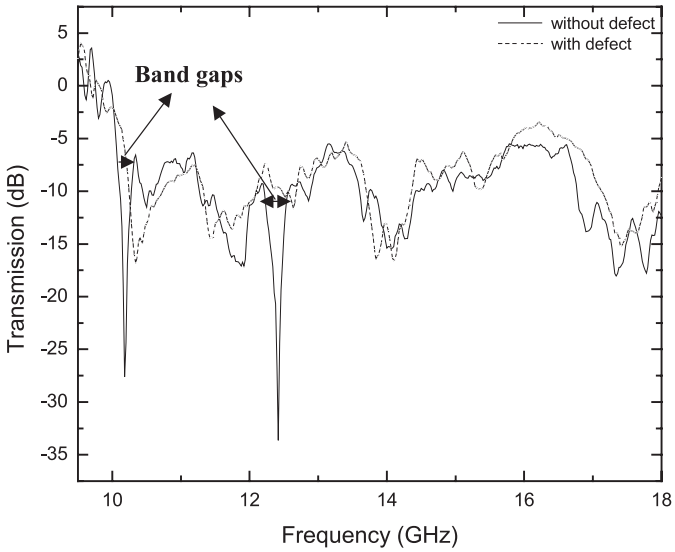

Fig. 3. The transmission spectrum of 2.5 cm square lattice with and without defects. The solid line corresponds to the spectrum without defects and the broken line corresponds to the spectrum with the defects at (3,4), (4,7), (5,7), (7,4), (8,2) and (8,8).

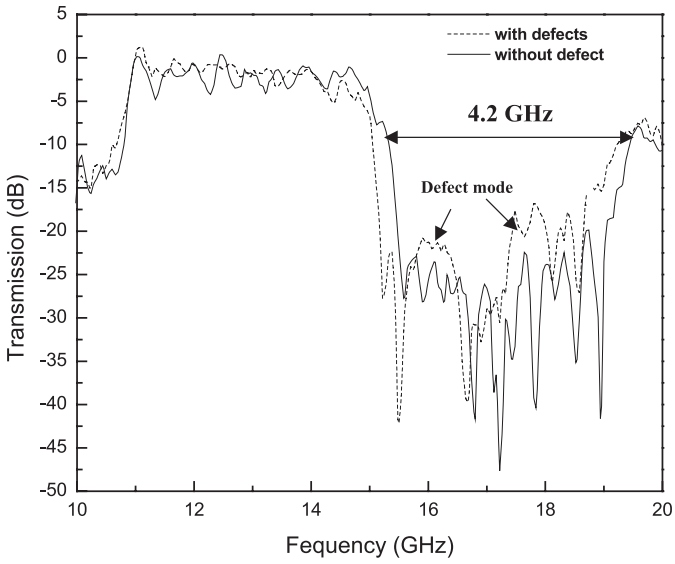

Fig. 4. The transmission spectrum of 1.4 cm square lattice with and without defects. The solid line corresponds to the spectrum without defects and the broken line corresponds to the spectrum with the defects at (4,3) and (4,8).

4.2 Triangular lattice

Figure 6 shows the arrangement of the triangular lattice. For a lattice constant of 2.5 cm, the spectrum, shown in Figure 7, shows two sharp gaps at 11.52 GHz and 16.08 GHz with a width around 0.29 GHz and 0.85 GHz respectively. The theory predicts a gap centered at 10.84 GHz with a gap width of 0.18 GHz.

Figure 8 gives the transmission spectrum for 1.4 cm lattice. It may be observed that the width of the gap is 2.6 GHz and is centered at 16.76 GHz whereas the

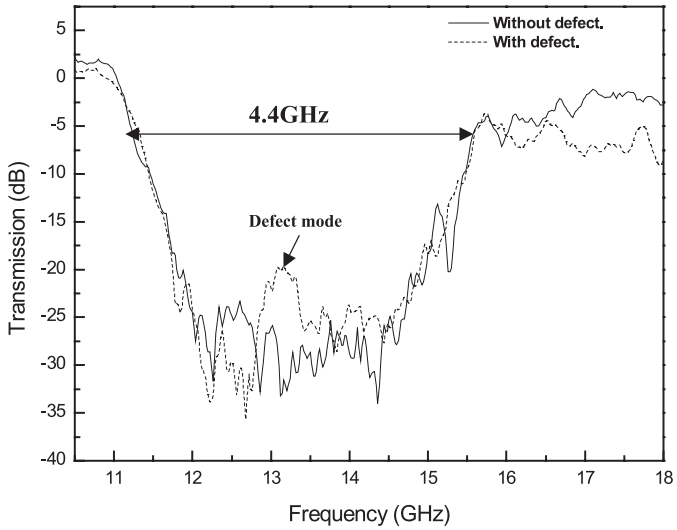

Fig. 5. The transmission spectrum of 0.9 cm square lattice with and without defects. The solid line corresponds to the spectrum without defects and the broken line corresponds to the spectrum with the defect at (2,5).

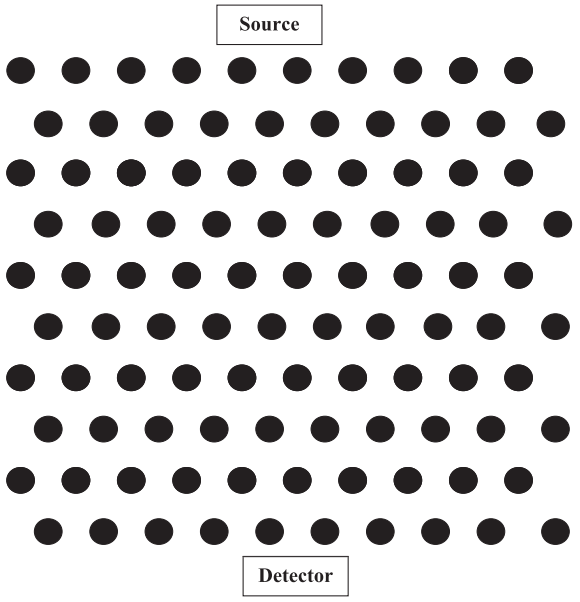

Fig. 6. The triangular lattice arrangement.

theoretical value of midgap frequency is 17.10 GHz with a gap width of 2.39 GHz.

With 0.9 cm lattice, the gap width is observed to be around 4.4 GHz centered at 14.58 GHz as shown in Figure 9. The band structure shows a band gap centered at 14.1 GHz with a gap width of 6.18 GHz in the Γ–M direction for this lattice structure as shown in Figure 2.

Plihal and Maradudin [18] reported that for a triangular lattice of dielectric contrast 5, in E-polarization, the band gap was centered at 5.99 GHz. The lattice spacing used in this case was 2.32 cm with a filling fraction of 0.169. As the dielectric constant in the our case was 5.5, and the lattice constants were different, the mid-gap frequencies for all the three structures of varying lattice

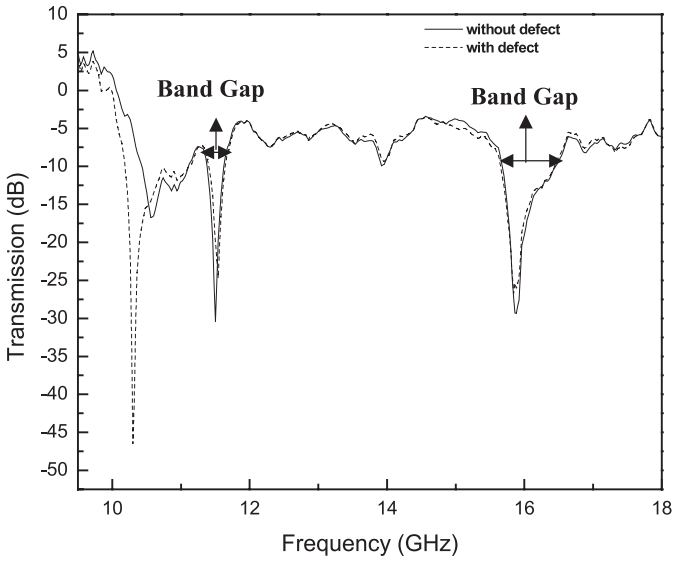

Fig. 7. The transmission spectrum of 2.5 cm triangular lattice with and without defects. The solid line corresponds to the spectrum without defects and the broken line corresponds to the spectrum with the defect at (4,6).

constants were calculated based on the values reported by Plihal and Maradudin [18] using the scaling methodology. For 2.5 cm lattice structure, the midgap frequency was expected to be at 5.26 GHz, which could not be observed experimentally within the scanned frequency range. For 1.4 cm lattice structure, the expected midgap frequency is 9.38 GHz, which also could not be observed within the scanned frequency range. For 0.9 cm lattice structure, the midgap frequency was observed to be at 14.58 GHz, which is in excellent agreement with the predicted value of 14.59 GHz.

Using the experimental results obtained in our case for 0.9 cm lattice spacing, scaling procedure was applied for 2.5 and 1.4 cm lattice spacings. It may be noted that the obtained midgap frequencies viz. 5.24 and 9.37 GHz for 2.5 and 1.4 cm lattice spacing respectively agree well with the values obtained with the scaling procedure based on the values reported by Plihal and Maradudin [18].

4.3 Square lattice with defects

The acceptor defects introduced for the 2.5 cm lattice resulted in an increase in the power levels of the gaps observed at 10.19 GHz and 12.39 GHz when compared to the pure structure as shown in Figure 3. It is expected that as an acceptor defect is introduced, there must be a mode in the gap region. But in this case, as the gap is sharp, it may not be possible to observe the defect mode. Figure 3 shows the disappearance of both gaps when six defects were introduced at (3,4), (4,7), (5,7), (7,4), (8,2), (8,8) [(m,n) represents mth row and nth column].

With the structure of lattice constant 1.4 cm, two extra modes appeared within the band gap, as shown in Figure 4, as defects were introduced at (4,3) and (4,8).

Table 1. Comparison between theoretical and experimental values for midgap frequencies in square and triangular lattices.

Lattice type	Spacing (cm)/ Filling fraction (%)	Theoretical value of midgap frequency (GHz) (Width in GHz)	Mid-gap frequency using scaling procedure (GHz)	Experimental value of the present work (GHz) (Width in GHz and Error % in mid-gap frequency)
Square lattice	2.5/0.022	10.58 (1.1)	---	10.19 (0.24) (<5%)
		---	---	12.32 (0.3)
	1.4/0.069	9.49	---	---
		16.62 (3.46)	---	17.42 (4.2) (<5%)
	0.9/0.166	12.90 (4.68)	13.45	13.39 (4.4) (<5%)
Triangular lattice	2.5/0.025	10.85 (0.18)	---	11.50 (0.29) (6%)
		---	---	16.10 (0.85)
	1.4/0.079	10.57	---	---
		17.10 (2.39)	---	16.80 (2.6) (<2%)
	0.9/0.192	14.10 (6.18)	14.59	14.58 (4.4) (<5%)

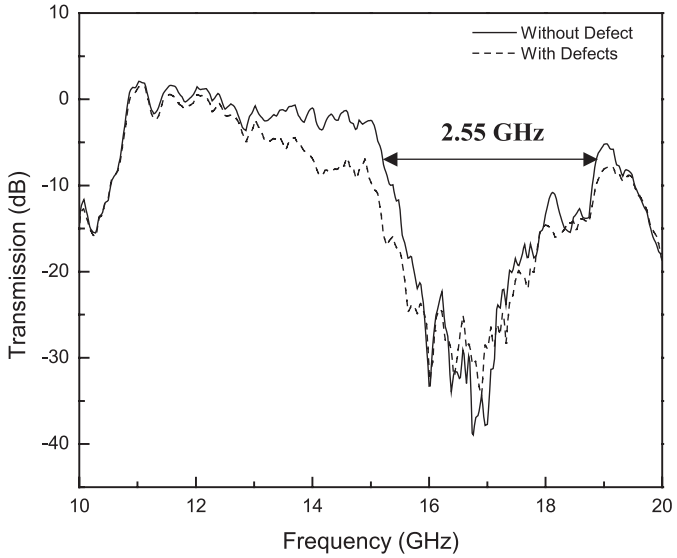

Fig. 8. The transmission spectrum of 1.4 cm triangular lattice with and without defects. The solid line corresponds to the spectrum without defects and the broken line corresponds to the spectrum with the defects at (1,7) and (2,4).

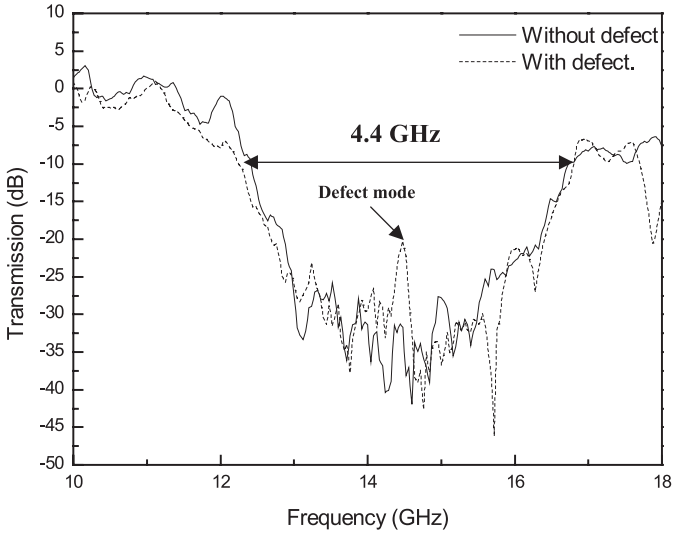

Fig. 9. The transmission spectrum of 0.9 cm triangular lattice with and without defects. The solid line corresponds to the spectrum without defects and the broken line corresponds to the spectrum with the defects at (4,7) and (5,5).

In 0.9 cm lattice constant structure, extra mode appeared within the band gap with the introduction of only one defect at (2,5) as shown in Figure 5. The width of the defect mode is around 1 GHz.

4.4 Triangular lattice with defects

Figure 7 gives the transmission spectrum of a triangular lattice of 2.5 cm lattice constant, when a defect was introduced at (4,6). The power level corresponding to the dip at 10.6 GHz decreased, indicating a pseudo gap. However, the gaps at 11.5 GHz and 16.1 GHz showed an increase in the power levels. With the structure of lattice constant 1.4 cm, no new mode was observed with the introduction of defects at (1,7) and (2,4), but an increase in power level by 5 dB was observed as shown in Figure 8. With the introduction of defects in the structure of lattice constant 0.9 cm at (4,7) and (5,5), an extra mode was observed (Fig. 9).

5 Discussion

Table 1 gives the comparison between the band gaps obtained using plane wave method, using scaling procedure and experimental values for the midgap frequencies for all the lattice constants. It may be observed that there is a good agreement between the theoretical and experimental values with respect to the mid-gap frequency whereas there is a poor agreement in terms of gap width. The

discrepancy in the width may be due to (a) the lossy nature of the samples and (b) finiteness of the structure. It is well known that plane wave method is suitable for infinite lattice structures and does not account for loss in the samples [15].

In general, it may be observed that for a higher filling fraction, the band gap becomes clearly visible. The fluctuations in the insertion loss within the band gap decreases for a triangular lattice compared to square as the triangular lattice has greater symmetry than that of square lattice. In most of the cases, the attenuation of power within the band gap was around 30 to 40 dB for a 10-layer structure. Beaky et al. [19] reported that the transmissivity decreases with increase in refractive index. The insertion loss of the structure is given as 10 log$n$ dB per lattice plane, where n is the refractive index. In the present case for $\varepsilon = 5.5$, the total insertion loss for 10 layers is 37 dB which agrees well with the experimental observation.

The defect modes that appeared for both square and triangular lattices are not as sharp as reported by McCall and Platzman [8]. A higher width for defect modes has also been reported for square alumina rods by Ozbay et al. [20]. In the present case, it has been suggested that the lossy nature of the dielectric increases the width of the defect mode (approximately 1 GHz). As it is well known that the plane wave method and the scaling methodology do not take into account the lossy nature of the sample, the width of the gap is a function of both dielectric contrast as well as loss factor of the sample. The lossy nature of the sample attenuates the electromagnetic radiation and depth of gap may not be as prominent as that of non-lossy structures.

Appearance of no extra modes due to the creation of defects in 1.4 cm triangular lattice indicates that apart from the filling fraction, the position of defects plays an important role in the appearance of the new modes. If the defect is near the source, there will be a drastic change in the spectrum while it may not be the case if it is near the detector. This is because the probability that the incoming waves will experience the sample rod near the source will be more when compared to that at the detector after undergoing scattering within the structure. For a larger structure, one may expect the position of the defect to play a less significant role.

6 Gap to mid-gap ratio

Villeneuve and Michel Piche [21] proposed theoretically that the gap to mid-gap ratio for 2-D cylindrical rods arranged in a square lattice saturates approximately at 0.1 for a dielectric contrast of 5. McCall and Platzman [8] obtained a gap to mid-gap ratio of 0.14 for a filling fraction of 0.45 for alumina rods arranged in square lattice. Both the above mentioned work dealt with very low loss dielectric samples.

Figures 10 and 11 show the variation of the gap to mid-gap ratio obtained using plane wave method as well as experimentally with filling fraction for square and triangular lattices respectively.

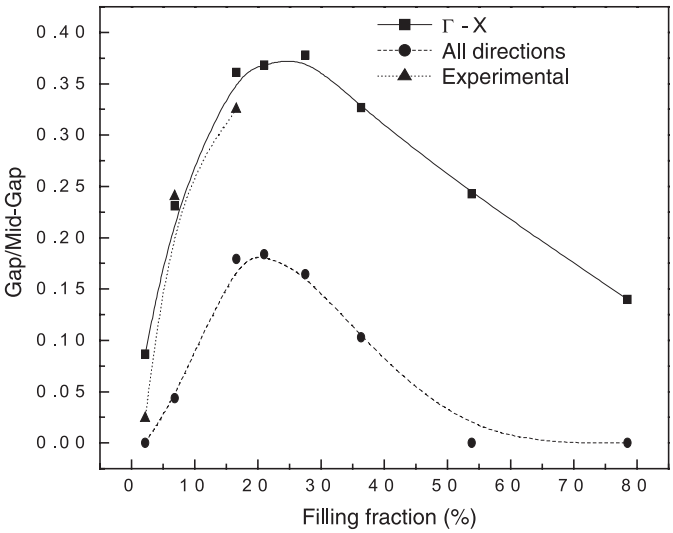

Fig. 10. The variation of gap to mid-gap ratio with filling fraction for square lattice.

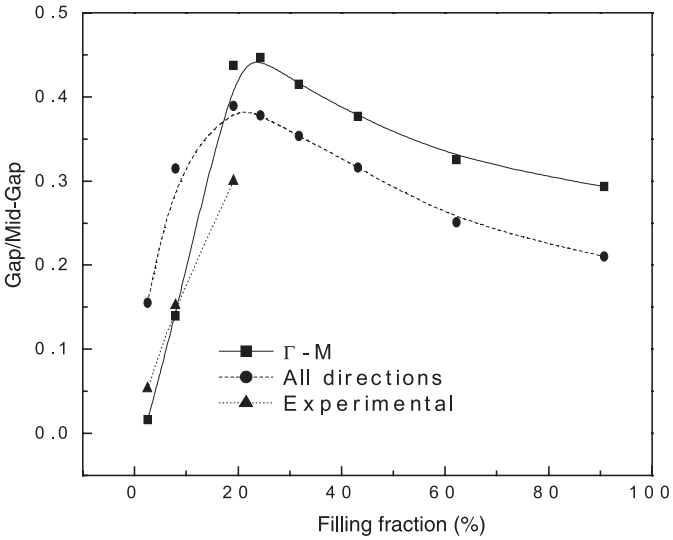

Fig. 11. The variation of gap to mid-gap ratio with filling fraction for triangular lattice.

It may be generally observed that the gap to mid-gap ratio increases with filling fraction till it reaches a maximum value and then decreases. In the case of square lattice, the complete band gap could not be observed for higher filling fraction whereas along the Γ-X direction, there is a finite value of the band gap observed. This means that when the receiver antenna is kept along Γ-X direction, it is still possible to get the band gap around 17 GHz. By rotating the antenna towards X-M direction, the gap narrows down and the gap width subsequently becomes zero. The optimum filling fractions are 0.21 and 0.28 for the complete band gap and band gap along Γ-X direction respectively. Along Γ-X direction, the optimum gap can be observed for 0.7 cm lattice spacing. It may be observed that the experimental results are following closely to that of Γ-X direction as expected.

In the case of triangular lattice, complete band gap indicates the optimum filling fraction around 0.19 pertaining to 0.9 cm lattice spacing whereas the band gap along Γ-M direction indicates the optimum filling fraction around 0.24 pertaining to 0.8 cm lattice spacing. The experimental results are following closely to that of Γ-M direction as expected.

Conclusions

The spectral response of the electromagnetic radiation between 10 and 20 GHz has been studied for square and triangular structures with three different spacings using cylindrical glass rods. The observed microwave band gaps for the above structures are compared with the theory and found to have good agreement. Though the material used in the present work is having some dielectric loss, the plane wave method suits well for predicting the position of midgap frequency of the band gap. The variation of gap to mid-gap ratio with filling fraction (for both square and triangular structures) indicates that for a specific dielectric material there may be a rapid increase in the ratio for smaller value of filling fraction and attains a peak at optimum filling fraction and decreases for higher filling fraction. It is also suggested that the loss tangent of the material and dielectric constant are responsible for the depth and width of the gap. For a finite lattice, the appearance of the defect mode is found to be position dependent. As the defect forms a local resonator, the width of the defect mode may be attributed to the loss tangent of the material.

The authors EDVN and GSB acknowledge the financial support provided by the Defence Research and Development Organization (DRDO), New Delhi, India and Council of Scientific and Industrial Research (CSIR), New Delhi, India respectively in the form of Junior Research Fellowship.

References

1. E. Yablonovitch, Phys. Rev. Lett. **58**, 2059 (1987)
2. S. John, R. Rangarajan, Phys. Rev. B **38**, 10101 (1988)
3. P.R. Villeneuve, M. Piche, Phys. Rev. B **46**, 4969 (1992)
4. E. Ozbay, B. Temelkuran, M. Sigalas, G. Tuttle, C.M. Soukoulis, K.M. Ho, Appl. Phys. Lett. **69**, 3797 (1996)
5. G.J. Schneider, S. Hanna, J.L. Davis, G.H. Watson, J. Appl. Phys. **90**, 2642 (2001)
6. B. Temelkuran, E. Ozbay, Appl. Phys. Lett. **74**, 486 (1999)
7. S. Satpathy, Z. Zhang, M.R. Salehpour, Phys. Rev. Lett. **64**, 1239 (1990)
8. S.L. McCall, P.M. Platzman, Phys. Rev. Lett. **67**, 2017 (1991)
9. J.D. Joannopoulos, R.D. Meade, J.N. Winn, *Photonic Crystals: Molding the Flow of Light* (Princeton University Press, Princeton, New Jersey, 1995)
10. E. Yablonovitch, T.J. Gmitter, Phys. Rev. Lett. **63**, 1950 (1989)
11. K.M. Leung, Y.F. Liu, Phys. Rev. B **41**, 10188 (1990)
12. M. Sigalas, C.M. Soukoulis, E.N. Economou, C.T. Chan, K.M. Ho, Phys. Rev. B **48**, 14121 (1993)
13. E. Yablonovitch, T.J. Gmitter, Phys. Rev. Lett. **67**, 3380 (1991)
14. P.R. Villeneuve, S. Fan, J.D. Joannopoulos, Phys. Rev. B **54**, 7837 (1996)
15. M. Sigalas, C.M. Soukoulis, C.T. Chan, K.M. Ho, Phys. Rev. B **49**, 11080 (1994)
16. M. Plihal, A. Shambrook, A.A. Maradudin, Optics Communications **80**, 199 (1991)
17. J.B. Pendry, A. MacKinnon, Phys. Rev. Lett. **69**, 2772 (1992)
18. M. Plihal, A.A. Maradudin, Phys. Rev. B **44**, 8565 (1991)
19. M.M. Beaky, J.B. Burk, H.O. Everitt, M.A. Haider, S. Venakides, IEEE Trans. Microwave Theory Tech. **47**, 2085 (1999)
20. E. Ozbay, G. Tuttle, J.S. McCalmont, M. Sigalas, R. Biswas, C.M. Soukoulis, K.M. Ho, Appl. Phys. Lett. **67**, 1969 (1995)
21. P.R. Villeneuve, M. Piche, Phys. Rev. B **46**, 4973 (1992)